RESEARCH ARTICLE

The spatial distribution and characterization of phosphorus and nitrogen in a water-carrying lake: a case study of Lake Jiaogang, China

Tianlun Han[1] · Kang Zhou[2] · Jiuling Li[3] · Ting Chen[1] · Xueting Xu[1] · Shuai Zhang[4] · Jianying Chao[1] · Ming Kong[1]

Abstract

The sources of P and N in water-carrying lakes include exogenous input and endogenous release. However, the influence of pollution from different sources on the dynamic distribution of N and P at the sediment-water interface in water-carrying lakes remains unclear. The objectives of this study were to investigate the differences in dynamic distribution characteristics of P compounds and N elements in Lake Jiaogang, a major water-carrying lake in eastern China. Four functional regions with different types of pollutant sources and different kinds of aquatic plants were selected to study the distribution of total P (TP), inorganic P, organic P, ammonium (NH_4^+–N), and nitrate (NO_3^-–N). The results revealed that regions with internal-source pollutants contained the highest concentration of TP, Ca–P, and Fe–P with high concentrations. L–P, Al–P, mostly organic P, and soluble reactive phosphorous (SRP), the region with internal-source pollutants were lower than that with the imported-source pollutant. The concentration of dissolved NH_4^+–N showed high in regions with imported-source pollutants, however, in regions with internal-source pollutants, the dissolved NO_3^-–N was with the highest concentration. Overall, P from upstream was still dominant in the sediments despite uptake by the aquatic plants. SRP showed high concentration in regions with imported-source pollutants due to the imported pollution and the improved bioavailability by plant root exudates. Feces and feed residues from aquatic livestock breeding resulted in the highest concentration of TN, NH_4^+–N, and dissolved NO_3^-–N in the sediments of the region with internal-source pollutants. High concentrations of dissolved NH_4^+–N were due to the input of N from imported source pollutants. This study provides insights into the contributions of P and N to the eutrophication of the water-carrying lake.

Keywords Water-carrying lake · Organic P · Inorganic P · NO_3^-–N · NH_4^+–N

✉ Ming Kong
   kongming@nies.org

1   Nanjing Institute of Environmental Sciences, Ministry of Ecology and Environment, Nanjing 210042, China

2   Chinese Research Academy of Environmental Sciences, National Engineering Laboratory for Lake Pollution, Control and Ecological Restoration, Beijing 100012, China

3   Australian Centre for Water and Environmental Biotechnology, The University of Queensland, St Lucia, Brisbane, QLD 4072, Australia

4   Jiangsu Key Laboratory of Atmospheric Environment Monitoring and Pollution Control (AEMPC), Collaborative Innovation Center of Atmospheric Environment and Equipment Technology (CIC-AEET), School of Environmental Science and Engineering, Nanjing University of Information Science & Technology, Nanjing 210044, China

Introduction

Large water-carrying lakes are served as water storage units worldwide. However, water-carrying lakes suffer from eutrophication, which causes deterioration of water quality and death of aquatic life. Phosphorus (P) and nitrogen (N) are recognized as the major nutrients for accelerating eutrophication (Li et al. 2021; Yu et al. 2016). Therefore, it is important to understand the chemical forms of P and N, the exchange, and biological effectiveness (Wan et al. 2020).

P consists of inorganic P and organic P in lake sediments and overlying water (Torres et al. 2014). The inorganic P includes exchangeable P, Al-bound, Fe-bound, and Ca-bound P. The organic P is composed of phospholipids, nucleic acids, sugar phosphates, inositol phosphates, and condensed P (Worsfold et al. 2008). Total P (TP), inorganic P, and organic P behave very differently in sediments and

overlying water (Onianwa et al. 2013; Torres et al. 2014). Nitrate (NO_3^-–N) and ammonium (NH_4^+–N) are the dominant components of inorganic N, causing eutrophication in the aquatic environment (Ren et al. 2020). The cooperative effects of P and N aggravate eutrophication.

The sources of P and N in water-carrying lakes include exogenous input and endogenous release (Fielding et al. 2020). The inflow rivers are the main source of water supply for water-carrying lakes (Feng et al. 2022). The increasingly developed industry, agriculture, and aquaculture have accumulated high concentrations of nutrient elements (Kong et al. 2021; Luo et al. 2021; Yang et al. 2015), which enter the inflow rivers under the action of soil erosion and surface runoff (Dai et al. 2022), and eventually flow into the lakes, resulting in the decline of water quality and ecological service function (Wan et al. 2020). In addition, previous studies have shown that the release of endogenous pollution could still keep lakes in a state of eutrophication for a long time when exogenous input was effectively controlled (Wang et al. 2021; Wu et al. 2021). However, the influence of pollution from different sources on the dynamic distribution of N and P at the sediment-water interface in water-carrying lakes remains unclear.

Lake Jiaogang, a large water-carrying lake in Anhui Province, China, plays an important role in the local development of the economy (Kong et al. 2021). In recent years, the water quality of Lake Jiaogang has been declining due to exogenous input and endogenous release. It was found that the water quality in September was the worst of the year according to the results of monthly monitoring for the water quality of Lake Jiaogang. In late September, the mature rice was harvested, and a large amount of discarded straw was placed near the three inflow rivers, Beizhongxi River, Nanzhongxin River, and Guangou River, and then washed into Lake Jiaogang under surface runoff. In addition, large areas of emergent plants and floating plants were distributed in the northern and western regions of Lake Jiaogang, respectively. Due to the decomposition of aquatic plant residues in September, a large number of N and P were released into the water, resulting in a decline in water quality. Besides, N and P were released from enclosure aquaculture which existed in the central area of Lake Jiaogang. Therefore, the distribution and characteristics of P compounds and N elements in the sediments and the overlying water of the lake will facilitate an understanding of the eutrophication risk to the aquatic environment.

This study aims to investigate the differences in dynamic distribution characteristics of P compounds and N elements in various regions with different pollution sources in the water-carrying lake. Four functional regions, including the eastern area without aquatic plants, the western region with floating plants, the northern area with emergent plants, and the middle area feeding aquatic livestock, were chosen to investigate P compounds and N compounds. Besides, TP, inorganic P, organic P, and N elements (including NO_3^-–N and NH_4^+–N) in sediments were analyzed. Moreover, concentrations of soluble reactive phosphorous (SRP), NO_3^-–N, and NH_4^+–N were quantified by high-resolution pore water equilibrates (HR-peeper) in the pore water and overlying water. Relationships of P and N compounds between the depth and sampling sites were revealed. These findings would advance our understanding of the risk evaluation of P and N compounds pollution in water-carrying lakes.

Material and methods

Study area

Lake Jiaogang locates in the northern part of the Anhui Province (32°35′–32°37′N, 116°34′–116°39′E) with a catchment area of 480 km^2, a mean depth of 1.2 to approximately 2.2 m, and a surface area of 37.5 km^2. The lake is classified as an important water-carrying lake and connects with the Huaihe River which is among the six largest water systems in China. Three large rivers, in the west and northeast directions of Lake Jiaogang, are discharged into the lake and result in the alluvial sediment. According to the previous field survey on the distribution of aquatic plants in Lake Jiaogang, large areas of emergent plants and floating plants were found in the northern and western regions of Lake Jiaogang, and the dominant species are *Nelumbo nucifera Gaertn.* and *Trapa bispinosa Roxb.*, respectively. In addition, the existence of enclosure aquaculture also was found in the central area of Lake Jiaogang, and the main species were *Hypophthalmichthys molitrix* and *Eriocheir sinensis*. Therefore, the lake was divided into four areas, such as emergent plant area (1[#] in Fig. 1, in the northern area of the lake, and with emergent aquatic plant), a floating plant area (2[#] in Fig. 1, in the west area of the lake, and culture floating plant), eastern area (3[#] in Fig. 1, in the eastern area of the lake, and without aquatic plant), and aquaculture area (4[#] in Fig. 1, in the middle area of the lake, was used to culture aquatic livestock).

Sample collection and preparation

In September 2020, a total number of eight sediment cores were collected from sites 1[#], 2[#], 3[#], and 4[#] in Lake Jiaogang using a gravity sampler, based on polycarbonate tubes with an inner diameter of 9.0 cm and a length of 40 cm. An overlying water sample (1 L) in each site was collected at the same time. All the samples were transported to the laboratory within 6 h. Four sediment cores (one for each site) were immediately adjusted to a length of 20 cm, with 10 cm of the overlying water, and then used to measure the concentration of SRP, NH_4^+–N, and NO_3^-–N at the sediment-water
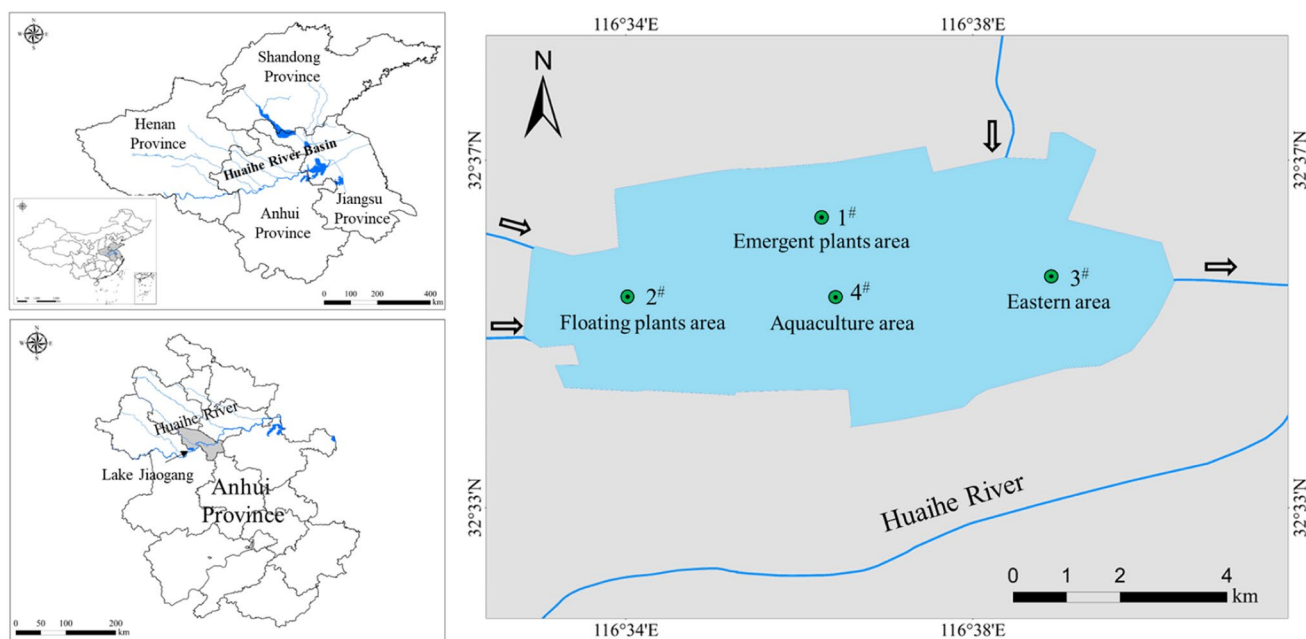
Fig. 1 Geographic locations of the Lake Jiaogang

interface (SWI) by HR-peeper (EasySensor Ltd. China) (Kong et al. 2021). The overlying water of the remaining four sediment cores was removed by siphoning and sliced immediately at 1 cm intervals for the upper part of the core (0–10 cm). All slices were then freeze dried, ground, passed through a 100-mesh sieve, sealed, and stored for analysis of P and N in sediments.

Analyses of P and N in sediments

TP was analyzed spectrophotometrically (Shimadzu, UV-2550) based on the molybdenum blue method and at 700 nm to measure the absorbance (Murpht and Riley 1962).

Inorganic P compounds in the sediments were extracted based on previous methods (Rydin 2000). The air-dried sediments (1.00 g) were added in centrifuge tubes (50 mL) and extracted sequentially with 0.11 M of $Na_2S_2O_4$ and $NaHCO_3$ (Fe–P), 1 M of NH_4Cl (L–P), 0.5 M of HCl (Ca–P), and 1 M of NaOH–P (Al–P). Residual P (Res-P) was calculated according to TP minus the total extracted P (Yin et al. 2017).

The organic P fractionation was measured according to the modified procedure (Ivanoff et al. 1998). The organic P was classified as non-labile, moderately labile, and labile sections. The non-labile section (Res-OP) was measured by ashing the solid residue by NaOH extraction for 1 h at 550 °C and subsequently dissolved in H_2SO_4 (1 M). Moderately organic P (HCl–OP) was extracted with HCl (1.0 M) and treated with NaOH (0.5 M). Acidification of NaOH (NaOH-OP) was extracted by conc. Fulvic-P was obtained by adding HCl (0.2 pH) to the sediment. The labile organic

P ($NaHCO_3$–OP) was extracted from the sediment with $NaHCO_3$ (0.5 M, pH 8.5) (Kong et al. 2020).

The sediment sample was sliced to analyze total N, NH_4^+–N, and NO_3^-–N at different depths. TN was measured after digestion by sulfuric acid and hydrogen peroxide. The concentrations of NH_4^+–N and NO_3^-–N were analyzed by extraction, oxidation, and spectrophotometry, respectively (Wang et al. 2021).

P and N in overlying and pore water

HR-peeper (EasySensor Ltd. China) was inserted into the sediments to obtain the concentrations of SRP and N at the SWI after equilibrium for 48 h (Yin et al. 2017). Pore water samples (150 mL) were collected by HR-peeper and diluted with 3% HNO_3 to 5 mL (Xu et al. 2012). The SRP in the solution was measured by a spectrophotometer (Shimadzu, UV-2550). The concentrations of NH_4^+–N and NO_3^-–N were measured by a Skalar flow-injection analyzer (Skalar Sanplus, The Netherlands).

Statistical analysis

The P, NH_4^+–N, and NO_3^-–N were divided into two different matrices, in which P, NH_4^+–N, and NO_3^-–N were set as environmental variables at different sampling sites. 9999 substitution times were obtained through the Mantel test (Mantel 1985). Multiple factor analysis (MFA) is a multivariable data analysis method for summarizing and visualizing complex data. The distance between objects and their

comprehensive relationship was determined by integrating the contributions and balancing the influences of each group of variables (Pagès 2002). Statistically significant was conducted by SPSS16.0 and Excel 2020.

Results and discussion

The variation of P in sediment and overlying water

TP, inorganic P, and organic P in sediments

To evaluate the risks of eutrophication in lakes, internal and imported sources of P should be tested (Yuan et al. 2014a). Sediment is regarded as one of the most important sources of internal P. In addition, the effect of the imported source from upstream on the spatial distribution and characterization of P in sediment should not be ignored. In this study, four functional regions, including the 1[#] (the region of imported source pollutant and culture emergent aquatic plants), 2[#] (region of imported source pollutant, culture floating plants), 3[#] (the region of downstream and without aquatic plants), and 4[#] (region of internal source pollutant and cultured aquatic livestock), were chosen to investigate the concentrations of TP (Fig. 2), inorganic P (Fig. 3), and organic P (Fig. 4).

The average concentrations of TP in sample 1[#], 2[#], 3[#], and 4[#] were 604.44 mg/kg, 689.74 mg/kg, 570.39 mg/kg, and 688.47 mg/kg, respectively. Pollutants imported from upstream might be resulted in a high concentration of TP in sample 1[#] and sample 2[#] despite adsorption by aquatic plants (Yuan et al. 2015). In addition, the high concentration in sample 4[#] was attributed to the aquatic livestock (Fig. 1). Considering TP is associated with different

chemical forms of P, inorganic P in the vertical profile of sediments was calculated (Fig. 3).

The vertical distribution of mostly inorganic P showed a decreased concentration with the increased depth in the four sample sites (Fig. 3). For instance, a decreased concentration of inorganic P, except for Fe–P, was observed with the increase of sediment depth in the sample 3[#] site (Fig. 3C). This result was similar to the previously reported result that mobile P content was decreases generally with the increase of sediment depth (Yin et al. 2017), which was mainly caused by decreased oxygen content and microbial activity.

Concentrations of inorganic P existed in a complicated relationship among the four sampling sites. Ca–P exhibited the overwhelming predominance in the sediments, with the average concentration of 225.94 mg/kg, 270.40 mg/kg, 226.79 mg/kg, and 324.12 mg/kg for sample 1[#], sample 2[#], sample 3[#], and sample 4[#], respectively, followed by Res-P Fe–P, Al–P, and LP (Fig. 3). Ca-P and Fe–P showed higher concentration in sample 4[#] compared with that of sample 1[#] and sample 2[#], which might be attributed to the aquatic livestock breeding and lack of adsorption by aquatic plants (Kong et al. 2021). In addition, high concentrations of TP in samples 2[#] and 4[#] also contributed to the results (Fig. 2). Specifically, the concentrations of L–P and Al–P in sample 4[#] were lower than those of sample 1[#] and sample 2[#]. For instance, the average concentrations of L–P were 2.17 mg/kg, 2.39 mg/kg, and 1.52 mg/kg in sample 1[#], sample 2[#], and sample 4[#], respectively. Pollution of the agricultural non-point source from three large rivers was discharged subsequently into the lake and buried in the sediments by physical, biological, and chemical actions (Kong et al. 2021; Tang et al. 2016; Wu et al. 2021). Besides, the bioavailability of P can be effectively improved by plant root exudates (Zhang
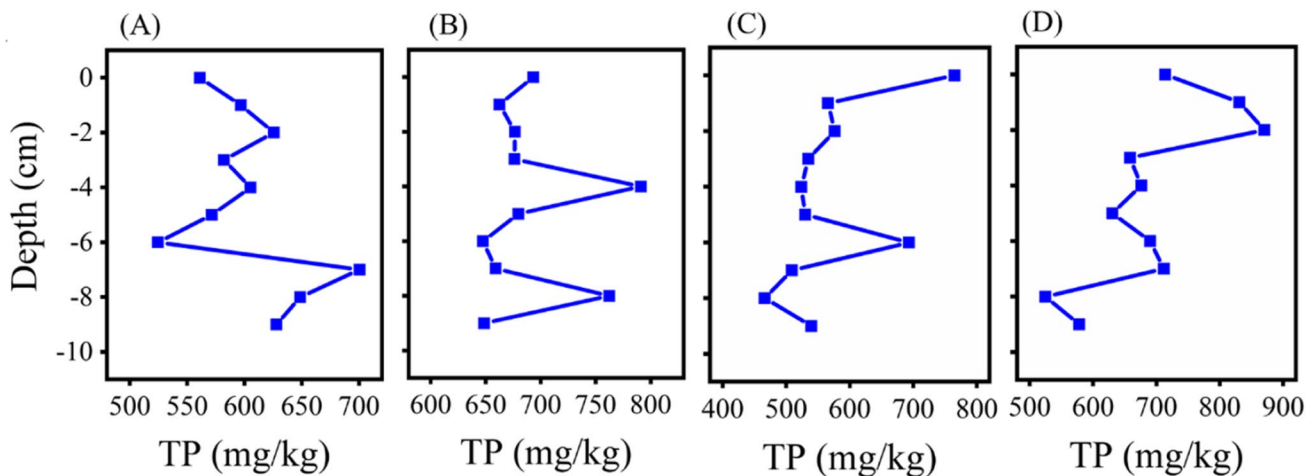

Fig. 2 The variation of TP in the vertical sediments. TP in 1[#] sampling site (**A**), 2[#] sampling site (**B**), 3[#] sampling site (**C**), and 4[#] sampling site (**D**), respectively
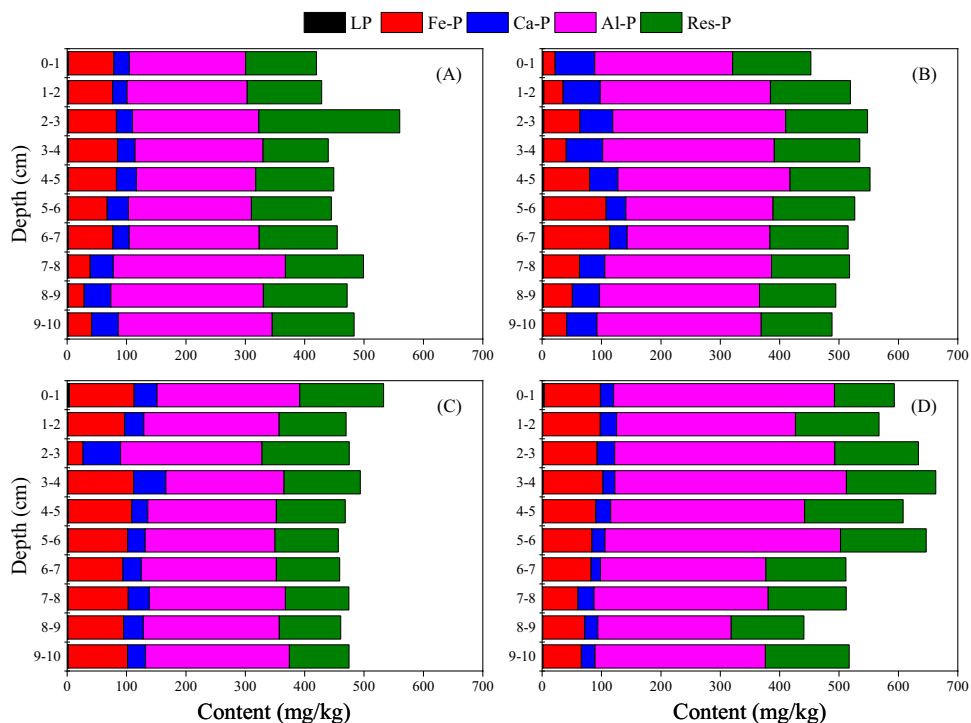
Fig. 3 Speciation of inorganic P in the vertical profile of sediments. Distributions of inorganic P in 1# sampling site (**A**), 2# sampling site (**B**), 3# sampling site (**C**), and 4# sampling site (**D**), respectively

Fig. 4 Speciation of organic P in the vertical profile of sediments. Distributions of organic P in 1# sampling site (**A**), 2# sampling site (**B**), 3# sampling site (**C**), and 4# sampling site (**D**), respectively
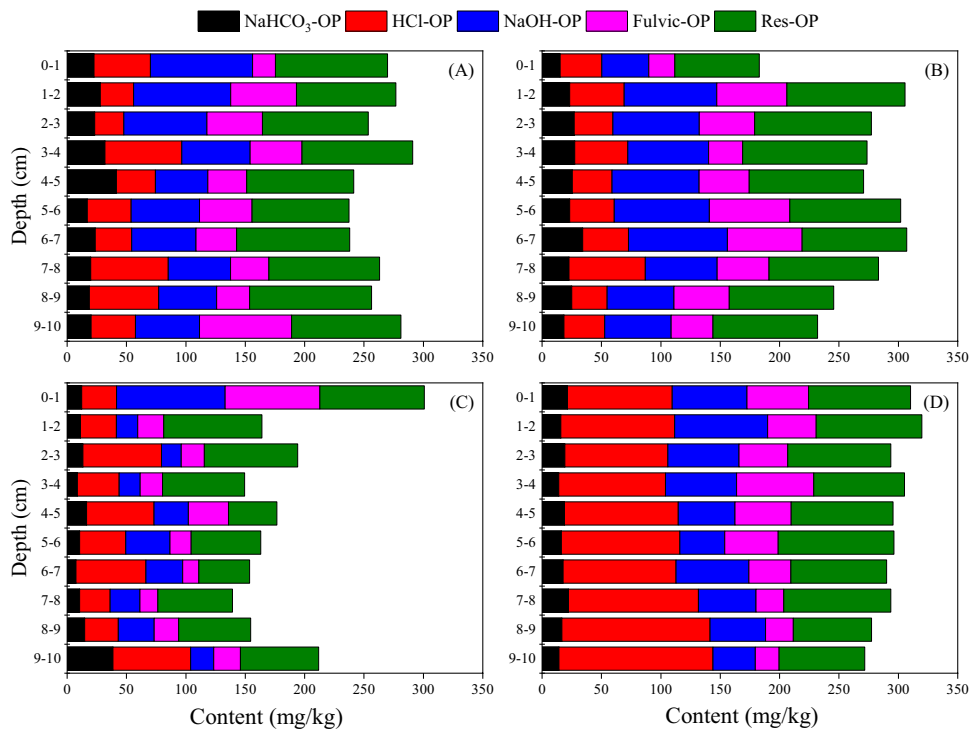
et al. 2021). Both factors resulted in the high concentrations of L–P and Al–P in sample 1# and sample 2#.

Organic P is an important component of TP and can be converted to inorganic P (Yuan et al. 2015). Concentrations of organic P, including NaHCO$_3$–OP, HCl–OP, NaOH–OP,

Fulvic-OP, and Res-OP, were shown in Fig. 4. Res-OP exhibited the highest concentration in the four sampling sites, followed by NaOH–OP, HCl–OP, fulvic-OP, and NaHCO$_3$–OP (Fig. 4). Most organic P, except for HCl–OP, showed lower concentration in sample 4# compared with that of sample

1# and sample 2#. For instance, the average concentrations of $NaHCO_3$–OP were 24.65 mg/L, 24.17 mg/L, and 17.60 mg/L in sample 1#, sample 2#, and sample 4#, respectively. Plant root exudates effectively facilitated the availability of P in sample 1# site and sample 2# site. Imported pollutions from upstream were discharged onto the lake and deposited subsequently in the sediments of sample 1# and sample 2# due to adsorption and immobilization (Dong et al. 2016; Kong et al. 2021). P, despite uptake by the aquatic plants, the input pollutions from upstream were still dominant in the sediments of sample 1# and sample 2#. Additionally, the concentrations of organic P in sample 4# showed higher compared with that of sample 3#. For example, the average concentration of HCl–OP in sample 4# was increased by a fold change of 2.37 compared to that of sample 3#.

The variation of SRP in pore and overlying water

SRP is the most readily bioavailable form of P for uptake by algal aquatic plants (Kong et al. 2020; Yuan et al., 2014b). The internal release of P transferred from the sediment to the water column based on physical and biochemical reactions was the important reason for the increased concentration of P in overlying water (Ren et al. 2020). The concentrations of SRP increased from overlying water (2–0 cm), peaked at around − 8 cm of sediments, and then slowly decreased along with the increased depth in the four sample sites (Fig. 5). Corresponding average concentrations of SRP in the pore water were higher than that of overlying water for each sampling site. The result indicated that SRP export from the sediments to the overlying water. In addition, SRP showed higher concentration in sample 1# or sample 2# (including in the overlying water and pore water) compared with that of sample 3# and sample 4#. Two factors, imported

pollution sources and improved bioavailability by plant root exudates, might result in the high concentrations of SRP in the two sites (Kong et al. 2021; Tang et al. 2016; Wu et al. 2021). Besides, the average concentration of SRP in sample 2# was higher than that of sample 1#. Compared with floating plants, emergent aquatic plants obtain a higher ability to uptake P, which was the main reason resulting in the above phenomenon (Zhang et al. 2021).

The variation of N in sediment and overlying water

The variation of N in sediment

The concentrations and depth distributions of TN were investigated in sediments (Fig. S2). The average concentrations of TN were 3712.40 mg/kg, 3853.55 mg/kg, 2685.06 mg/kg, and 4253.60 mg/kg in the sediments of samples 1#, 2#, 3#, and 4#, respectively. Feces and feed residues from the aquatic livestock breeding were discharged into the lake and subsequently deposited in the sediments, which resulted in the highest concentration of TN in the sediments of sample 4# among all four samples. In addition, pollutants from upstream might result in a higher concentration of TN in the sediments of sample 1# and sample 2# than that of sample 3#, which might attribute to the imported pollution from upstream also adsorption by aquatic plants.

Different chemical forms of N are associated with TN, such as NH_4^+–N and NO_3^-–N, in the vertical profile of sediments, were investigated (Fig. 6). The vertical distribution of NH_4^+–N and NO_3^-–N, showed an increased concentration with the increased depth in the four sample sites (Fig. 6). Compared with NO_3^-–N, NH_4^+–N exhibited the overwhelming predominance in the sediments with the average concentrations of 110.66 mg/kg, 76.27 mg/
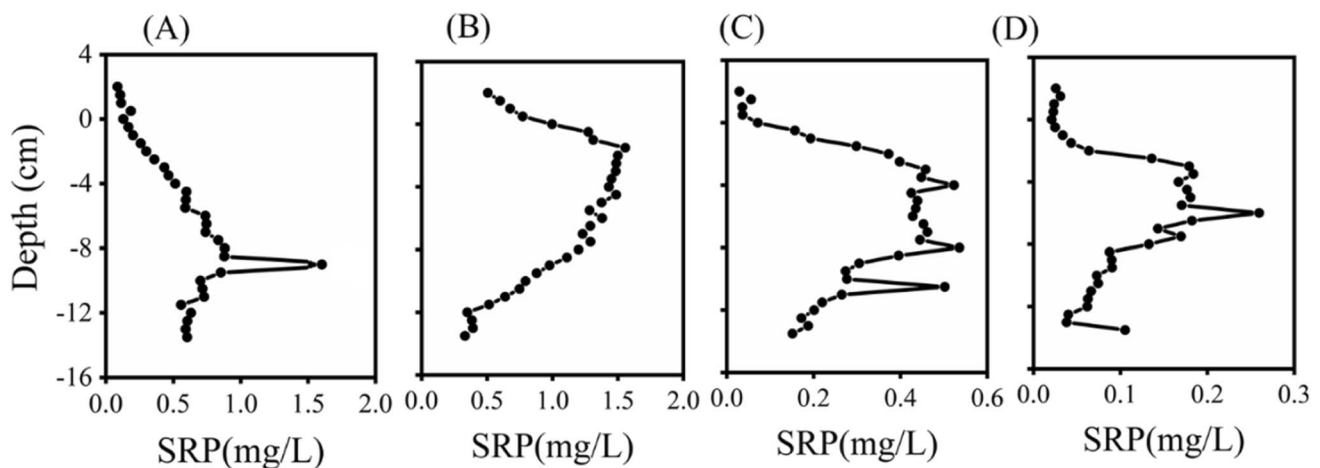
Fig. 5 The variation of P was tested by HR-peeper in the pore and overlying water. Distributions of P in 1# sampling site (**A**), 2# sampling site (**B**), 3# sampling site (**C**), and 4# sampling site (**D**), respectively

Fig. 6 The variation of NH_4^+–N and NO_3^-–N in the vertical sediments. The variation of NH_4^+–N in 1[#] sampling site (**A**), 2[#] sampling site (**B**), 3[#] sampling site (**C**), and 4[#] sampling site (**D**), respectively. The variation of NO_3^-–N in 1[#] sampling site (**E**), 2[#] sampling site (**F**), 3[#] sampling site (**G**), and 4[#] sampling site (**H**), respectively.
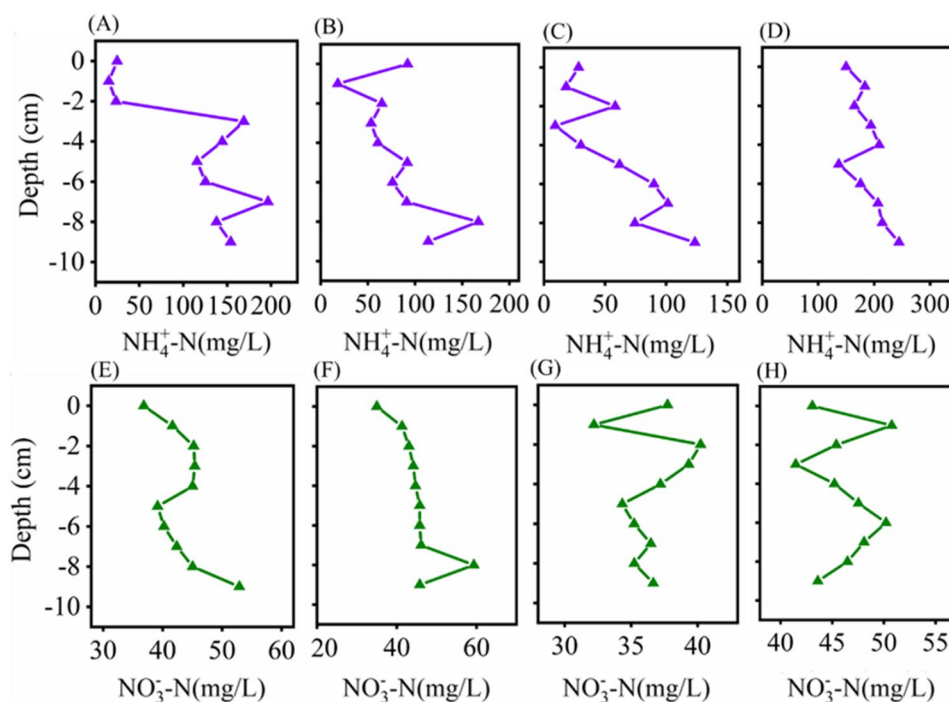
kg, 61.54 mg/kg, and 187.90 mg/kg for sample 1[#], sample 2[#], sample 3[#], and sample 4[#], respectively. NH_4^+–N can be transformed from other nitrogen forms by ammonifiers through ammonification (Li et al. 2020; Yu et al. 2010). In this sense, inorganic nitrogen in sediment always showed high concentrations of NH_4^+–N (Li et al. 2020). Specifically, NH_4^+–N showed a higher concentration in sample 4[#] compared with that of sample 1[#], sample 2[#], and sample 3[#]. Feces and feed residues were generated and deposited and increased the content of NH_4^+–N in the sediments of sample 4[#]. In addition, the concentrations of NH_4^+–N in sample 1[#] and sample 2[#] showed higher than that of sample 3[#]. The result indicated that the input N from upstream was still dominated despite uptake by the aquatic plants in the sediments of sample 1[#] and sample 2[#]. The concentrations of downstream (sample 3[#]) NH_4^+–N were decreased due to sedimentation, adsorption, and degradation.

The variation of N in pore and overlying water

A high heterogeneous nature is shown in sediments, especially at the SWI (Ren et al. 2020). High-resolution measurements of N in the pore and overlying water should be tested. An HR-peeper was developed for rapid sampling of dissolved NH_4^+–N and NO_3^-–N in the pore and overlying water (Fig. 7). NH_4^+–N showed the highest concentration in the sediments of sample 4[#] compared with that of other samples (Fig. 6). However, the concentrations of dissolved NH_4^+–N showed higher in sample 1[#] and sample 2[#] compared with that of sample 3[#] and sample 4[#]. These results

manifested that the content of TN or NH_4^+–N in sediment does not determine the dissolved NH_4^+–N in the pore water. Input N from upstream might result in the high concentrations of dissolved NH_4^+–N in the two sites. Furthermore, oxidation-reduction potential can be altered due to the release and absorption of oxygen by aquatic macrophyte roots, which influences the concentrations of dissolved NH_4^+–N in interstitial water fluxes at the SWI (Bai et al. 2012; Lizotte and Moore 2017). The average concentrations of dissolved NH_4^+–N in the pore water were higher than that of overlying water for the sampling sites, which indicated that dissolved NH_4^+–N were exported from the sediments to the overlying water. The concentration of dissolved oxygen in overlying water is usually higher than that in sediment, especially in the presence of aquatic plants, which results in partial NH_4^+–N being transformed into NO_3^-–N through nitrification (Bai et al. 2012; Yu et al. 2016).

Corresponding average concentrations of dissolved NO_3^-–N are different with NH_4^+–N in the pore and overlying water. The concentrations of dissolved NO_3^-–N showed higher in sample 3[#] (0.21 mg/L) and sample 4[#] (0.18 mg/L) compared with that of sample 1[#] (0.11 mg/L) and sample 2[#] (0.06 mg/L). Specifically, the average concentrations of dissolved NO_3^-–N in overlying water were higher than that of the pore water for sample 1[#] and sample 2[#]. NO_3^-–N was transformed by NH_4^+–N through nitrification at the SWI in the presence of aquatic plants (Bai et al. 2012; Yu et al. 2016). Compared with the area without aquatic plants, floating plants and emergent aquatic plants cultured in the two areas obtain a higher ability to adsorb dissolved NO_3^-–N,

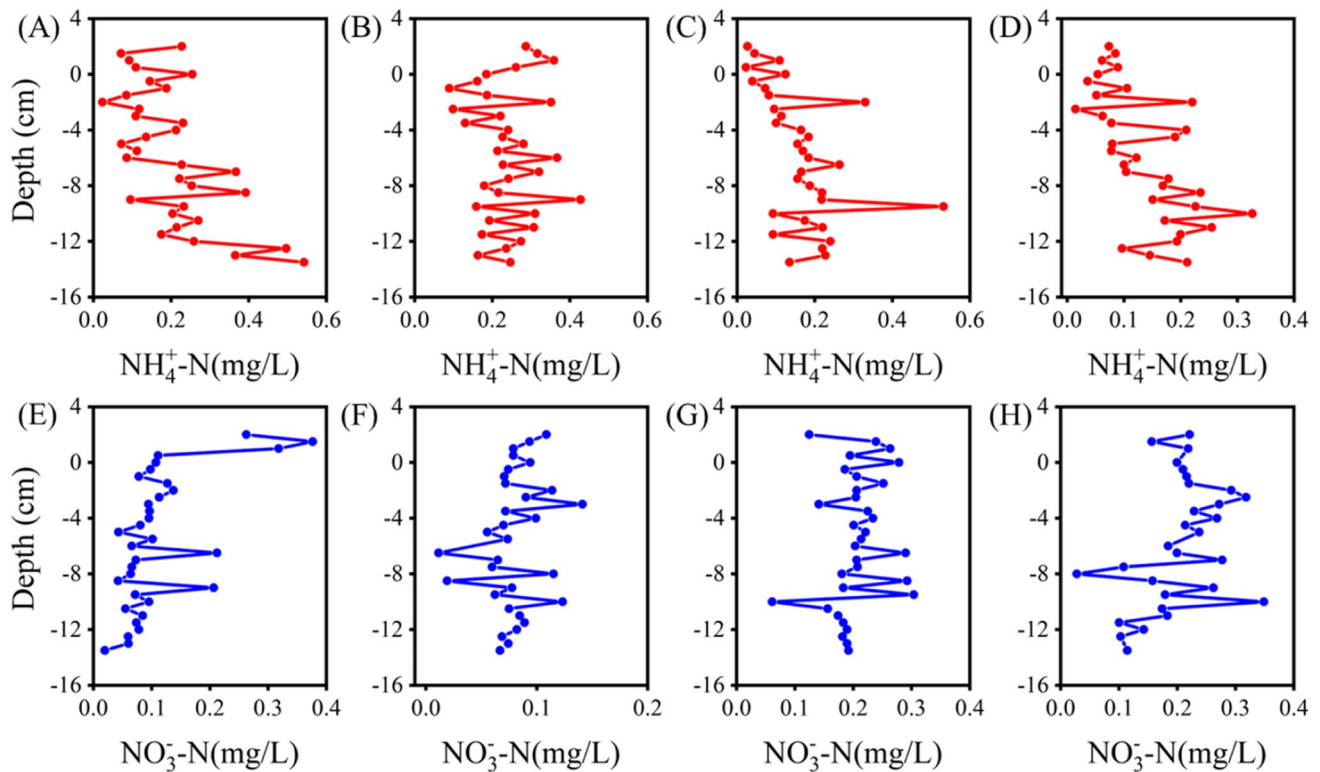**Fig. 7** The variation of NH_4^+–N and NO_3^-–N in the pore and overlying water. The variation of NH_4^+–N in 1[#] sampling site (**A**), 2[#] sampling site, (**B**) 3[#] sampling site (**C**), and 4[#] sampling site (**D**), respectively. The variation of NO_3^-–N in 1[#] sampling site (**E**), 2[#] sampling site (**F**), 3[#] sampling site (**G**), and 4[#] sampling site (**H**), respectively

which might be the main reason result in the above phenomenon (Kong et al. 2021). In addition, released N from an internal source might also enhance the high concentrations of dissolved NO_3^-–N in sample 3[#] and sample 4[#].

Correlation between P and N

In order to explore the relationship between N and P at different points and depths, MFA was carried out for different sampling sites, depths, sampling types, and variable factors (N and P) (Fig. 8). Figure 8A shows the correlation between variable groups and dimensions. After dimensionality reduction, 48.97% of the total variance, including 28.91% of the horizontal axis and 20.06% of the vertical axis, indicated that the analysis was credible. The concentrations of N (e.g., NH_4^+–N and NO_3^-–N) and P (e.g., organic P and inorganic P) in sediment were correlated with the vertical axis, while concentrations of P (e.g., organic P and inorganic P) in sediment, SRP and N (e.g., NH_4^+–N and NO_3^-–N) in the pore and overlying water correlated with the horizontal axis. Specifically, SRP and N in the pore and overlying water were contributed to the horizontal axis, which was 0.77 and 0.51, respectively. The organic P and inorganic P in the sediments

showed similar contributions to the horizontal axis (e.g., 0.60 and 0.49) and vertical axis (e.g., 0.47 and 0.47).

Feature decomposition was performed for all standardized variable sets, and principal component analysis (PCA) was performed for all quantitative variable factors (N and P). The variable factors in each variable group were divided by the characteristic roots of the first axis of their PCA to obtain the normalized variable sets, and all the normalized variable sets were summarized into a big data figure (Fig. 8B). Each set of variables was projected onto a PCA ordination graph. The common structure and differences of the dataset were assessed by the ordination graph of variables. There was a high correlation between the concentrations of P (e.g., organic P and inorganic P) and MFA in sediments, specifically, which were 0.73 and 0.67, respectively. However, low correlations were found between the concentrations of variable factors (e.g., NH_4^+–N and NO_3^-–N in the sediments or the pore and overlying water, and SRP) and MFA (Fig. 8B).

Significantly positive correlations were detected among the concentrations of organic P, except for HCl–OP (Fig. 8C) ($p < 0.05$). However, complicated relationships among the inorganic P. For example, significantly positive correlations were observed between the concentrations of L–P and Al–P, and these two kinds of P were
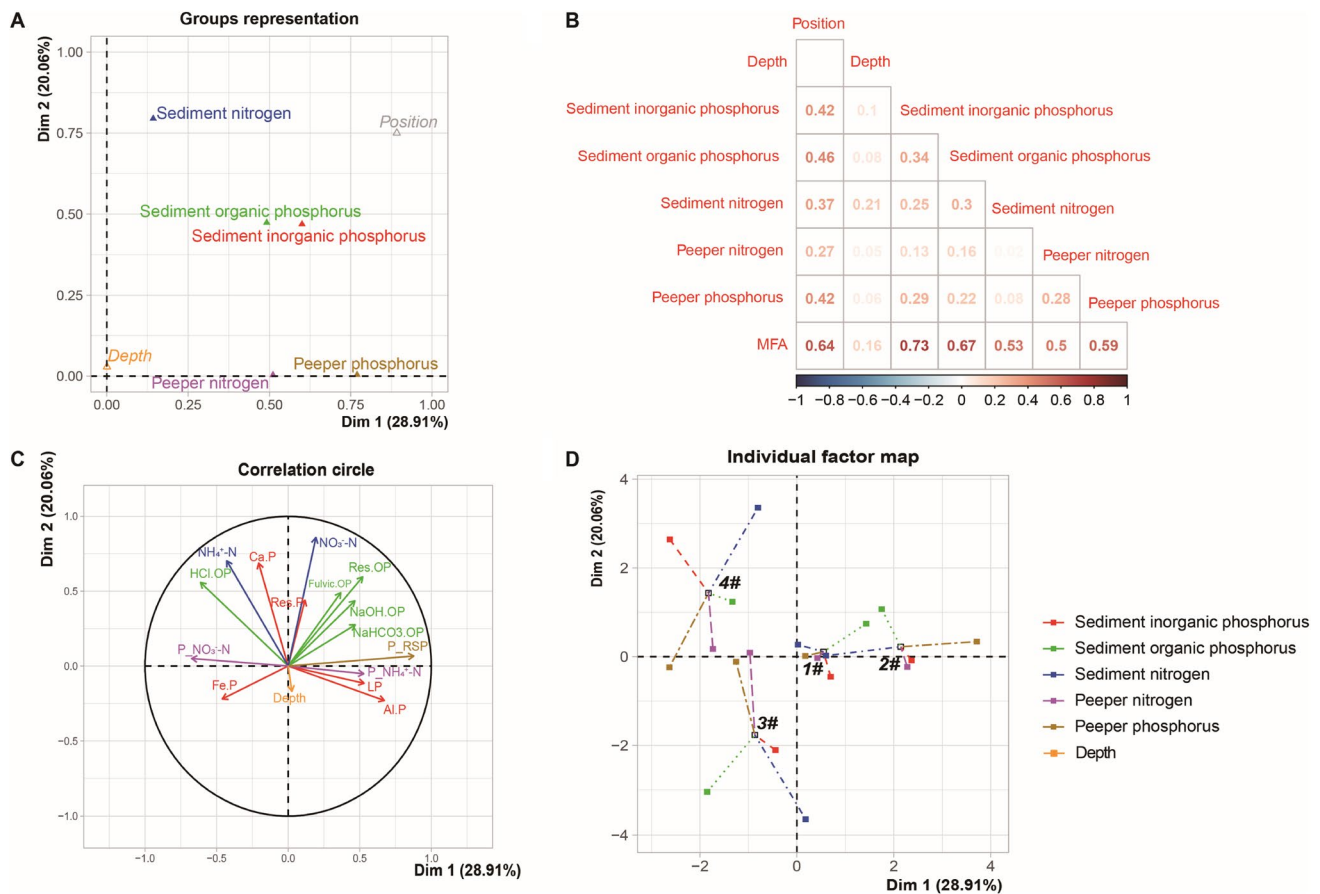
Fig. 8 Relationships of the P and N in the Lake Jiaogang (1#, 2#, 3#, and 4#). **A** The correlation between groups of variables and dimensions, **B** the MFA correlation between groups of variables and dimensions, **C** the correlation between variables (N and P) and their contribution to dimensions (an acute angle between variables is a positive correlation, and the length direction is the contribution to the two axis), **D** the contribution of variable factors (N and P) to the differences of sampling sites. The point position (e.g., 1#, 2#, 3#, and 4#) and depth (unit: cm) were defined as position and depth, respectively, and set to supplementary groups. LP, Fe–P, Al–P, Ca–P, and Res-P were defined as sediment inorganic phosphorus variable groups. NaHCO$_3$–OP, HCl–OP, NaOH–OP, Fulvic-OP, and Res-OP were defined as sediment organic phosphorus variable groups. NH$_4$–N and NO$_3^-$–N were defined as sediment nitrogen variable groups. N and P in peeper were defined as peeper nitrogen and peeper phosphorus variable groups, respectively

negative-correlated with Fe–P, Ca–P, and Res-P ($p <$ 0.05). Besides, the concentrations of SRP were positive-correlated with the concentrations of most organic P (organic P, excluding HCl–OP) and inorganic P (L–P and Al–P) ($p <$ 0.05). Corresponding to N, the concentrations of NH$_4^+$–N were positive-correlated with the concentrations of NO$_3^-$–N in the sediments, however, negative correlations were observed between the concentrations of these two kinds of N in the pore and overlying water ($p <$ 0.05). In summary, based on the contribution values of variable factors (N and P) to the four sampling sites, it was revealed that sample 1# and sample 2# were in the same dimension, and sample 3# and sample 3# were in separate dimensions (Fig. 8D). These results indicated that concentrations of P and N in sampling sites 1# and 2# were similar. Nevertheless, the two sampling sites were significantly different from those of sampling sites 3# and 4#.

Conclusion

The results indicated that TP, Ca–P, and Fe–P showed higher concentration in sample 4# compared with that of sample 1# and sample 2#. L–P, Al–P, mostly organic P, and SRP in sample 4# were lower than that of sample 1# and sample 2#. Despite uptake by the aquatic plants, P from upstream showed high concentrations in the sediments. In addition, SRP in the pore water was higher than that of overlying water for each sampling site. High concentrations of SRP were shown in regions with imported-source pollutants might be due to the imported pollution and the improved bioavailability of plant root exudates. The vertical distribution of NH$_4^+$–N and NO$_3^-$–N showed an increased concentration with the increased depth in the four sample sites. NH$_4^+$–N showed a higher concentration in sample 4# compared with that of sample 1#, sample 2#, and sample 3#. Compared with

that of sample 3# and sample 4#, the concentrations of dissolved NH_4^+–N showed higher in sample 1# and sample 2# due to the input of N from imported source pollutants. The concentrations of dissolved NO_3^-–N in sample 3# and sample 4# were higher than that of sample 1# and sample 2#. The concentrations of dissolved NH_4^+–N in the pore water were higher than that of overlying water for the sampling sites. Dissolved NO_3^-–N in overlying water was higher than that of the pore water for the samples 1# and 2#. Aquatic livestock breeding resulted in the highest concentration of NH_4^+–N and dissolved NO_3^-–N with internal-source pollutants. The relationships between N and P at different sampling points and depths were explored.

Declarations

References

Bai X, Chen K, Ren K, Huang W, Chen X (2012) Impacts of four emergent macrophytes on sediment nutrient loading. J Freshwater Ecol 27:481–493

Dai D, Lei K, Wang R, Lv XB, Hu JX, Sun MD (2022) Evaluation of river restoration efforts and a sharp decrease in surface runoff for water quality improvement in North China. Environ Res Lett 17

Dong DP, Zhang TX, Zhang DY, Wang QY, Li DF, Wang GX (2016) Characteristics of organic phosphorus fractions in the sediments of the black water aggregation in Lake Taihu. Huan jing ke xue 37:4194–4202

Feng LK, Zhang J, Fan JL, Wei LL, He SF, Wu HM (2022) Tracing dissolved organic matter in inflowing rivers of Nansi Lake as a storage reservoir: implications for water-quality control. Chemosphere 286:131624

Fielding JJ, Croudace IW, Kemp AE, Pearce RB, Cotterill CJ, Langdon P, Avery R (2020) Tracing lake pollution, eutrophication and partial recovery from the sediments of Windermere, UK, using geochemistry and sediment microfabrics. Sci Total Environ 722:137745

Ivanoff DB, Reddy KR, Robinson S (1998) Chemical fractionation of organic phosphorus in selected histosols. Soil Sci 163:36–45

Kong M, Liu F, Tao Y, Wang P, Wang C, Zhang YM (2020) First attempt for in situ capping with lanthanum modified bentonite (LMB) on the immobilization and transformation of organic phosphorus at the sediment-water interface. Sci Total Environ 741:140342

Kong M, Zhu YZ, Han TL, Zhang S, Li JL, Xu XT, Chao JY, Zhang YM, Gao YX (2021) Interactions of heavy metal elements across sediment-water interface in Lake Jiaogang. Environ Pollut 286:117578

Li C, Ding SM, Ma X, Chen MS, Zhong ZL, Zhang Y, Ren MY, Zhang M, Yang LY, Rong N, Wang Y (2021) O-2 distribution and dynamics in the rhizosphere of Phragmites australis, and implications for nutrient removal in sediments. Environ Pollut 287:9

Li XJ, Zhao YP, Wang GX, Han RM, Dang XY, Li ZR, Ren JF, Gao CX (2020) Sedimentary nitrogen fractions and source assignment from different inflows to a receiving lake. Water Supply 20:1950–1964

Lizotte RE, Moore MT (2017) Effectiveness of emergent and submergent aquatic plants in mitigating a nitrogen-permethrin mixture. Chem Ecol 33:420–433

Luo Y, Dong Z, Liu Y, Zhong D, Jiang F, Wang X (2021) Safety design for water-carrying lake flood control based on copula function: a case study of the Hongze Lake, China. J Hydrol 597

Mantel N (1985) Propriety of the Mantel - Haenszel variance for the log rank test. Biometrika 72:471–472

Murpht J, Riley JP (1962) A modified single solution method for the determination ofphosphate in natural waters. Anal Chim Acta 27:31–36

Onianwa PC, Oputu OU, Oladiran OE, Olujimi OO (2013) Distribution and speciation of phosphorus in sediments of rivers in Ibadan, South-Western Nigeria. Chem Spec Bioavailab 25:24–33

Pagès J (2002) Analyse factorielle multiple appliquée aux variables qualitatives et aux données mixtes. Rev Stat Appl 50:5–37

Rydin E (2000) Potentially mobile phosphorus in Lake Erken sediment. Water Res 34:2037–2042

Ren MY, Ding SM, Shi D, Zhong ZL, Cao JX, Yang LY, Tsang DCW, Wang D, Zhao DH, Wang Y (2020) A new DGT technique comprised in a hybrid sensor for the simultaneous measurement of ammonium, nitrate, phosphorus and dissolved oxygen. Sci Total Environ 725:138447

Tang WZ, Duan SH, Shan BQ, Zhang H, Zhang WQ, Zhao Y, Zhang C (2016) Concentrations, diffusive fluxes and toxicity of heavy metals in pore water of the Fuyang River, Haihe Basin. Ecotoxicol Environ Saf 127:80–86

Torres IC, Turner BL, Reddy KR (2014) The chemical nature of phosphorus in subtropical lake sediments. Aquat Geochem 20:437–457

Wan J, Yuan X, Han L, Ye H, Yang X (2020) Characteristics and distribution of organic phosphorus fractions in the surface sediments of the inflow rivers around Hongze Lake, China. Int J Env Res Pub He 17

Wang WH, Wang Y, Zhao KX, Zhu Z, Han XY (2021) Active and synchronous control of nitrogen and organic matter release from sediments induced with calcium peroxide. Sci Total Environ 802:149855

Worsfold PJ, Monbet P, Tappin AD, Fitzsimons MF, Stiles DA, McKelvie ID (2008) Characterisation and quantification of organic phosphorus and organic nitrogen components in aquatic systems: a review. Anal Chim Acta 624:37–58

Wu ZS, Lai XJ, Li KY (2021) Water quality assessment of rivers in Lake Chaohu Basin (China) using water quality index. Ecol Indic 121

Xu D, Wu W, Ding SM, Sun Q, Zhang C (2012) A high-resolution dialysis technique for rapid determination of dissolved reactive phosphate and ferrous iron in pore water of sediments. Sci Total Environ 421:245–252

Yang Y, Cai YM, Bai YY, Chen WP, Yang XC (2015) Land use pattern change and regional sustainability evaluation of wetland in Jiaogang Lake. Huan Jing Ke Xue 36:2320–2326

Yin HB, Du Y, Kong M, Liu C (2017) Interactions of riverine suspended particulate matter with phosphorus inactivation agents across sediment-water interface and the implications for eutrophic lake restoration. Chem Eng J 327:150–161

Yu H, Zhang WB, Lu SY, Yan SW, Hu RJ, Chen L, Zhang LL, Yu JP (2010) Spatial distribution characteristics of surface sediments nutrients in Lake Hongze and their pollution status evaluation. Huan jing ke xue 31:961–968

Yu J, Fan C, Zhong J, Zhang Y, Wang C, Zhang L (2016) Evaluation of in situ simulated dredging to reduce internal nitrogen flux across the sediment-water interface in Lake Taihu, China. Environ Pollut 214:866–877

Yuan H, An S, Shen J, Liu E (2014a) The characteristic and environmental pollution records of phosphorus species in different trophic regions of Taihu Lake, China. Environ Earth Sci 71:783–792

Yuan H, Liu E, Pan W, Geng Q, An S (2014b) Species and characteristics of organic phosphorus in surface sediments of northwest region of Taihu Lake, eastern China. Clean-Soil Air Water 42:1518–1525

Yuan HZ, Pan W, Ren LJ, Liu EF, Shen J, Geng QF, An SQ (2015) Species and biogeochemical cycles of organic phosphorus in sediments from a river with different aquatic plants located in Huaihe River watershed, China. Int J Phytoremediat 17:215–221

Zhang X, Zhen W, Jensen HS, Reitzel K, Jeppesen E, Liu Z (2021) The combined effects of macrophytes (Vallisneria denseserrulata) and a lanthanum-modified bentonite on water quality of shallow eutrophic lakes: a mesocosm study. Environ Pollut 277:116720